IEEE Access
Multidisciplinary | Rapid Review | Open Access Journal

Date of publication xxxx 00, 0000, date of current version xxxx 00, 0000.

Digital Object Identifier 10.1109/ACCESS.2017.Doi Number

Multi-climate factors and the preceding growth stage of vegetation co-regulated the variation of the end of growing season in Northeast Inner Mongolia, China

Wendu Rina[1,2], Gang Bao[1,2], Siqin Tong[1,3], Yuhai Bao[1,2], Yin Shan[1,2], Xiaojun Huang[1,2], Hong Ying[4] and Lingtong Du[5,6]

[1] College of Geographical Science, Inner Mongolia Normal University, Hohhot 010022, China;
[2] Inner Mongolia Key Laboratory of Remote Sensing and Geographic Information Systems, Inner Mongolia Normal University, Hohhot 010022, China
[3] Inner Mongolia Key Laboratory of Disaster and Ecological Security on the Mongolian Plateau, Inner Mongolia Normal University, Hohhot 010022, China
[4] Key Laboratory of Geographical Processes and Ecological Security in Changbai Mountains, Ministry of Education, School of Geographical Sciences, Northeast Normal University, Changchun 130024, China
[5] Breeding Base for State Key Laboratory of Land Degradation and Ecological Restoration in Northwest China, Ningxia University, Yinchuan 750021, China
[6] Key Laboratory for Restoration and Reconstruction of Degraded Ecosystem in Northwest China of Ministry of Education, Ningxia University, Yinchuan 750021, China

Corresponding author: Gang Bao (baogang@imnu.edu.cn) and Siqin Tong (tongsq223@imnu.edu.cn)

This research was supported by the National Natural Science Foundation of China (61631011, 41961144019, 41861021, 42061070), Graduate Research and Innovation Foundation of Inner Mongolia Autonomous Region (CXJJB20012), and the Opening Foundation of Key Laboratory for Restoration and Reconstruction of Degraded Ecosystem in Northwest China of Ministry of Education, Ningxia University (2018KF03).

ABSTRACT The end of growing season (EOS) is an effective indicator of annual vegetation growth. Previous studies have revealed the dynamics of the EOS with climate change, while the influence of vegetation growth in preceding stage and peak of growing season (POS) on the EOS has not been thoroughly documented. In this study, we used four smoothing methods to obtain EOS dates from the Normalized Difference Vegetation Index (NDVI) in northeast Inner Mongolia (NIM) between 2001–2017, assessed the differences in the spatiotemporal variations of the EOS obtained by the four smoothing methods, and then investigated the impacts of climate factors, summer/ autumn vegetation growth and POS on the EOS. The results showed that the EOS dates obtained with different smoothing methods were broadly consistent in terms of their spatial patterns and temporal trends. In terms of climate factors, the EOS was driven mainly by preseason precipitation for the majority of vegetation types and advanced with increasing precipitation. For the steppe, both minimum temperature (T_{min}) and relative humidity (RHU) played the most important roles in regulating the variation of EOS which was delayed with an increase in T_{min} and reduction in RHU. Furthermore, our study found an earlier POS and vigorous vegetation growth in summer would jointly advance the steppe EOS, but these relationships were the opposite of each other in meadow and forest regions. Interestingly, the EOS of NIM was more related with vegetation growth in the most recent period before the EOS. This study highlights the importance of ecological processes in the preceding growth stage for understanding the dynamics of EOS.

INDEX TERMS End of growing season, Northeast Inner Mongolia, Climate change, Peak of growing season, Preceding growth stage of vegetation

I. INTRODUCTION

Global warming continuously affects the structure and function of terrestrial ecosystems [1], [2]. As a fundamental indicator of ecological processes, land surface vegetation exerts a feedback on the climate system by regulating hydrothermal circulation [3] and carbon exchange at the Earth's surface [4], [5]. Phenology, i.e., the events that occur during plant growth and their development rhythm[6], [7], has become the focus of global change studies due it being an essential element of ecosystem models [8]–[10]. Numerous

This article has been accepted for publication in a future issue of this journal, but has not been fully edited. Content may change prior to final publication. Citation information: DOI 10.1109/ACCESS.2020.3043788, IEEE Access

studies have reported that a delayed end of growing season (EOS) is one of the major determinants of a prolonged growing season in the middle and high latitudes of the Northern Hemisphere [11], [12], which will result in an increase in the carbon storage of terrestrial ecosystems [13]. However, some researchers have reported that a later EOS would also lead to the loss of carbon by ecosystem respiration during autumn warming [14]. This suggests that a thorough monitoring of the EOS could expand our understanding of the terrestrial ecosystem carbon cycle.

The Normalized Difference Vegetation Index (NDVI), which is derived from satellite remote sensing, has been widely applied in the estimation of land surface phenology in recent years [15]–[17]. Various methods have been developed to extract the EOS from the NDVI [18], which generally involve two main steps: elimination of the noise in NDVI data and identification of the EOS [19], [20]. In the first step, several methods, such as the Savitzky–Golay filter [21], Fourier decomposition [22], and logistic function [23], have been adopted to eliminate the noise in NDVI data, which is due to contamination by cloud cover, seasonal snow, and atmospheric variability. In the next step, the predetermined thresholds and the inflection point methods are frequently used to identify the EOS on the NDVI curve [6], [24].Previous studies have concluded that the EOS identification method has a substantial impact on the spatiotemporal pattern of the EOS [19], [25]. However, the impact of noise smoothing methods on the magnitude and trend of the EOS remain uncertain. Although some studies have revealed distinctions among the available smoothing methods [26], [27], they were mainly based on the use of one-year data to assess the performance of smoothing methods at test points. Only a few of them have quantitatively characterized the influence of various filters on the interannual changes of the EOS [27].

Most studies have attempted to explain the changes in EOS through daily mean temperature and precipitation [20], [28]. However, the temperature has experienced faster warming during the nighttime than daytime over the past five decades[29], which has an asymmetric effect on phenological parameters [30]. In addition, some studies have found that an increase in T_{max} has a greater impact on the start of growing season (SOS) than T_{min} in the Northern Hemisphere, which is mainly caused by the combined effects of sunshine duration and daytime temperature [2]. However, Chew *et al.* [31] proposed that the temperature effects on the flowering time were mediated mainly by sunshine duration during spring and summer days, but the nighttime temperature was found to play a pivotal role in temperature effects as days shorten in autumn in the phenology model. Yang *et al.* [32] revealed the asymmetric responses of the EOS to T_{min} and T_{max} in the Tibetan Plateau. However, the contribution of T_{min} versus T_{max} on the EOS in temperate ecosystems is not well known and how the temperature and sunshine duration co-determine the EOS also remains uncertain. Moreover, relative humidity could trigger rainfall regardless of dry or wet soil conditions [33], which will induce the stomatal opening of plants and improve photosynthetic efficiency [34]. Therefore, it should be included in assessments to determine if humidity triggers the EOS. As the main part of the growing season, the variation of the summer vegetation growth has a residual effect on the EOS [35], [36]. Previous studies have quantified the summer vegetation growth as the average NDVI of summer and found that the summer vegetation growth increases the cost of soil water overconsumption which then advances the EOS in the Tibetan Plateau [35]. In contrast, the summer vegetation growth could delay the EOS in the Yellow River Basin, because the increasing precipitation induced by vegetation activity is sufficient to offset enhanced evapotranspiration [36]. These conflicting results imply the complex responses of biomes under different climate conditions, and none of these studies quantified the relative importance of the vegetation growth in each preceding month in determining the EOS. Furthermore, the peak of growing season (POS) of plant activity, referring to the timing of the highest degree of photosynthetic capacity, directly affects carbon uptake and water consumption [37]. Evidence from several studies has noted that the POS has shifted towards spring throughout the majority of the Northern Hemisphere mid-latitudes [12] and the earlier occurrence of POS results in vigorous vegetation activity through enhanced carbon assimilation early in the growing season [38], [39]. Yet, little is known about the impact of change in the POS on the EOS of different biome types.

Northeast Inner Mongolia (NIM) is located in a climate transitional zone, including a range of terrestrial ecosystems along the moisture gradient from semi-arid steppe and semi-humid forest, and contains a cropland region. This region contains one of the world's four largest natural pastures and the important forest area of the Mongolian Plateau, which extends over the Greater Khingan Mountains, with a low intensity of human disturbance [40]. The extensive diversity of vegetation and highly vulnerable ecosystems in the region, especially their phenological shifts, are very sensitive to global warming [41]. Consequently, it is an ideal region for investigating the response of EOS variations to climate and the preceding growth stage of vegetation. The main objectives of our study were to: (i) assess the influence of different NDVI smoothing methods on interannual changes in the EOS; (ii) investigate how the EOS changed over the NIM from 2001 to 2017; (iii) systematically analyze the effects of multiple preseason climate factors on the EOS variation; and (iv) explore the impact of the preceding growth stage of vegetation before the EOS on the interannual variation of the EOS, especially for different plant functional types. The results of this study improve our understanding of how the multiple climate factors and the preceding growth stage of vegetation jointly affect the EOS in temperate ecosystems. It would be useful to consider these mechanisms in future carbon cycle models.

II. MATERIALS AND METHODS

A. STUDY AREA

This article has been accepted for publication in a future issue of this journal, but has not been fully edited. Content may change prior to final publication. Citation information: DOI 10.1109/ACCESS.2020.3043788, IEEE Access

The NIM region extends from approximately 47°05′–53° 20′N and 115°31′–126°04′E, covering a total area of about 2.53 × 105 km^2. The elevation of NIM ranges from 167 m in the east to 1,675 m in the central mountains. The annual total precipitation varies widely from 195 mm in the west to 510 mm in the east, with most rainfall received in June to August. The vegetation across the NIM exhibits an extensive natural diversity along with precipitation and topography gradients, and can be divided into four major types: steppe, meadow, forest, and cropland (Fig. 1). The steppe mainly occurs in western parts of NIM, with an annual mean temperature range of -3-0°C. Forest is widely distributed in the Greater Khingan Mountains across the central part of the study area, with an annual mean temperature range of -5 to -2°C. The transition zone between steppe and forest mainly contains meadows. Cropland areas are spread across the eastern part of NIM and are scattered among mountains toward the west, with an annual mean temperature range of 0-2°C.

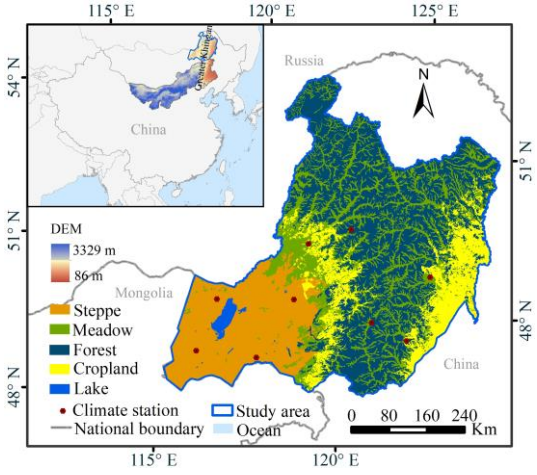

FIGURE 1. Geographic location, distribution of elevation, vegetation types, and meteorological stations of northeast Inner Mongolia (NIM).

B. DATASETS

Moderate-resolution Imaging Spectro-radiometer (MODIS) NDVI datasets spanning the period from 2001–2017 were used to retrieve the land surface phenology metrics across the study area. The 16-day maximum-value composite NDVI data (MOD13Q1) at a spatial resolution of 250 km were pre-processed and released by the Level-1 and Atmosphere Archive and Distribution System (LAADS) of the National Aeronautics and Space Administration (NASA) (http://ladsweb.nascom.nasa.gov/). We further processed the NDVI data, i.e., mosaicking image scenes, converting the geographic coordinate system, and clipping by boundaries. Climate records for the period of 2001–2017 were obtained from the China Meteorological Data Service Center of the China Meteorological Administration (http://cdc.cma.gov.cn). The climatic datasets were collected from nine meteorological stations (Fig. 1) and then spatial interpolation data was obtained using the Kriging method [42], including the daily minimum temperature (T_{min}), daily maximum temperature (T_{max}), sunshine duration (SSD), relative humidity (RHU), and precipitation. The vegetation types were obtained from a vegetation map of Inner Mongolia, with a scale of 1:1000000. The data was collected in 2000 and was further grouped into steppe, meadow, forest, and cropland. Previous studies have shown that the cropland area has increased substantially in Northeast Inner Mongolia since 2000 [43]. Hence, the range of cropland in this study was updated based on the 2010 MODIS Land Cover Type Product (MCD12C1), and the remaining regions retained their original properties.

C. DETERMINATION OF THE PHENOLOGY PARAMETERS FROM THE NDVI

Original NDVI data is usually affected by residual noise despite being processed by the standard maximum value compositing (MVC) technique [44]. Therefore, we adopted the harmonic analysis of time series (HANTS), asymmetrical Gaussian function (AG), double logistic function model (DL), and Savitzky Golay (SG) filtering methods to smooth the NDVI time-series data before identifying the EOS dates (Table S1). Furthermore, we applied the cumulative NDVI based logistic regression curve method to determine the EOS from smoothed NDVI data (Table S2). This method was developed by Hou, *et al.* [45] and is widely used for retrieving phenological phases. First, we calculated the cumulative NDVI based on the smoothed NDVI data and then fitted the cumulative NDVI to interpolate daily NDVI values using the logistic model. Second, we obtained the change rate of fitted logistic NDVI curves. Finally, we specified the EOS as the time when the change in the curvature rate reached its minimum value (Fig. S1b). The summer average NDVI (June, July, and August) and September NDVI represented the preceding growth stage of vegetation and was used to identify the impact on the EOS. In addition, we used the sixth-degree polynomial function [46] to interpolate daily NDVI from the 16-day NDVI, and then the timing of the occurrence of maximum NDVI in summer was defined as the POS date (Fig. S1a).

D. ANALYSES

The Theil-Sen median trend analysis and Mann-Kendall test method [47] were used to assess the spatial characteristics of EOS trends in each pixel. To further investigate the differences in EOS trends among different vegetation types, we calculated the spatial average EOS of each vegetation type to examine the overall trends. In addition, to understand the effects of the potential driving factors on the EOS, Pearson correlation coefficients [55] were calculated and a t-test was performed to assess the relationships between the EOS and both preseason climate factors and the preceding growth stages of vegetation (June, July, August, and September NDVI, summer average NDVI and POS). Here, based on the multiyear (2001–2017) spatial average EOS for each vegetation type, we determined that the last day of September could be regarded as the start of the preseason in the steppe, meadow, and cropland regions, while the last day in mid-October was considered to be the

This article has been accepted for publication in a future issue of this journal, but has not been fully edited. Content may change prior to final publication. Citation information: DOI 10.1109/ACCESS.2020.3043788, IEEE Access

start of the preseason in the forest area. Furthermore, we used stepped intervals of 10 days to calculate the mean T_{min} for each of 15 periods, with durations ranging from 10–150 days (i.e., 10, 20, 30, …., 150) for each pixel. The same procedure was executed for the other climate factors. Hence, the preseason length of each climate factor was defined as the period which had the largest correlation coefficient for the relationship with the EOS.

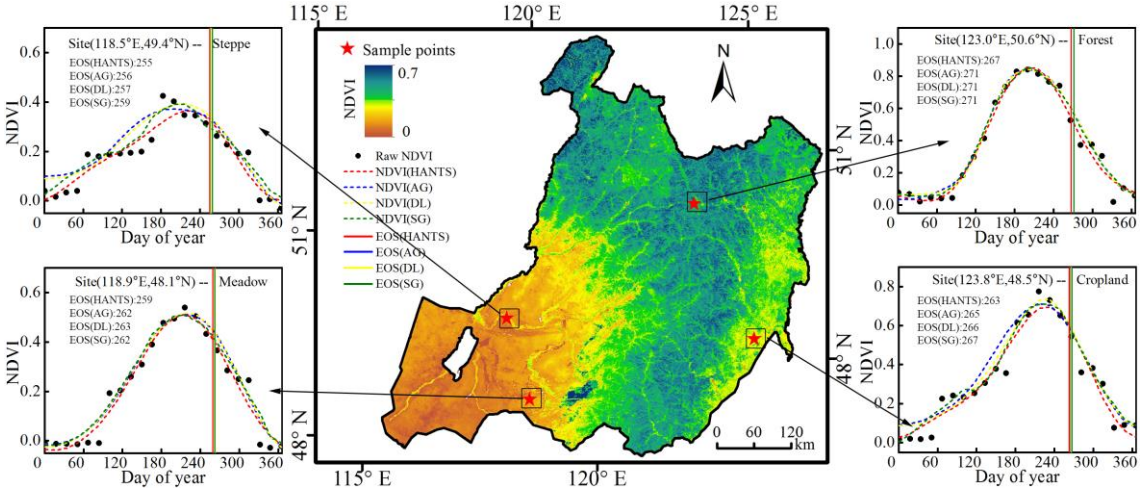

FIGURE 2. The spatial distribution of the multiyear averaged Normalized Difference Vegetation Index (NDVI). The four enlarged panels show the curves smoothed by four different methods (harmonic analysis of time series (HANTS), asymmetric Gaussian (AG) function, double logistic (DL) function, Savitzky-Golay (SG) filter) and the corresponding end of growing season (EOS). The sample pixels are in steppe (top left), meadow (bottom left), forest (top right), and cropland (bottom right)

III. RESULTS

A. ANALYSIS OF THE DIFFERENT SMOOTHING METHODS TO EXTRACT THE EOS

The performance of four smoothing methods and the corresponding EOS at four sample sites selected from 2006 are displayed in Fig 2, in which each inset represents a vegetation type. It was observed that all denoising methods were effective for smoothing the time series of NDVI data. Comparing four EOS dates obtained using the different smoothing methods, we found that the dates obtained with AG, DL, and SG were extremely similar (within 3 days) for most biomes, and were even in the same day in the forest region. Moreover, the EOS date obtained with HANTS was usually earlier than the date obtained with the other three methods, which was four days earlier in most of the forest area. The spatial distribution of the multiyear average EOS, which was derived from the four filtered NDVI values during the period of 2001–2017 is shown in Fig. 3. The spatial patterns of the four EOS dates were extremely consistent with each other. The earliest EOS dates were located in the southwest and east of the study area, whereas the later EOS dates were mainly identified in the central mountain region. We calculated the standard deviation (SD) of the EOS obtained with the four smoothing methods (Fig. 3f). Nearly 90% of the total pixels had SDs of less than 4 days, while only 10% of all pixels had SDs of more than 4 days, of which 2% of pixels had SDs of more than 6 days. In contrast, the SDs were smaller in the steppe area than in the other biomes (Fig. S2).

A comparison of the multiyear average EOS for each biome at regional scales (Fig. 4a) revealed a good resemblance among AG, DL and SG method. However, the EOS obtained from the NDVI smoothed by HANTS was approximately 5 days earlier than the value obtained using the other methods for the entire study area and the different vegetation types (Fig. 4a). Fig 4b-f shows the interannual variations of the EOS estimated from the different smoothed NDVI data and their mean values during 2001–2017 for different plant functional types. The curves of interannual changes of the EOS based on the different methods were in good agreement with each other (Fig. 4b) and the slope values were almost the same across the whole study area (Table S3). Consistent results were obtained for all vegetation types (Fig. 4c-f). Overall, the EOS results obtained using the different methods displayed similar characteristics, and therefore, we used the average value of the four EOS dates in the following analysis.

This article has been accepted for publication in a future issue of this journal, but has not been fully edited. Content may change prior to final publication. Citation information: DOI 10.1109/ACCESS.2020.3043788, IEEE Access

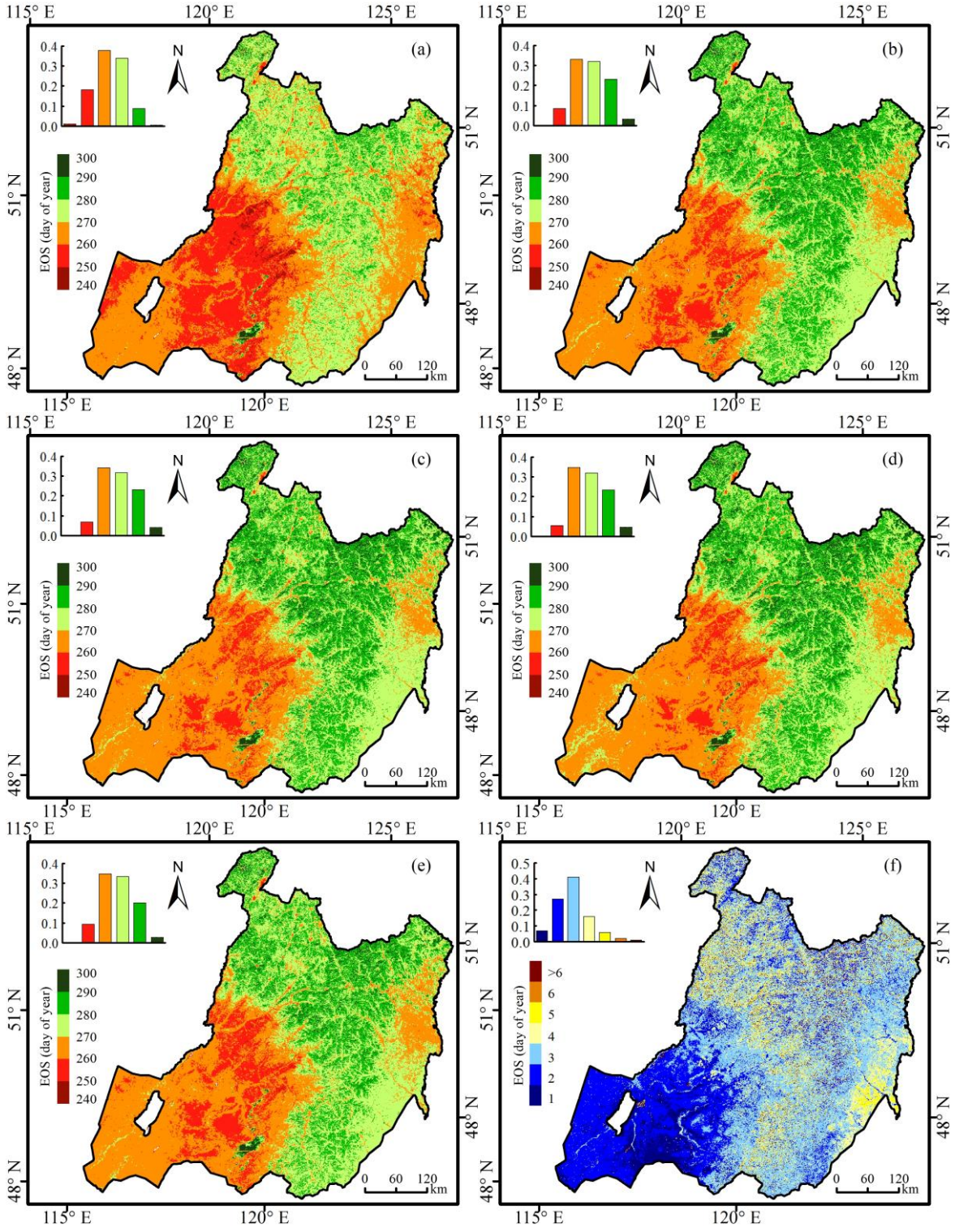

FIGURE 3. **The spatial pattern of EOS in the study area obtained with the four smoothing methods and their average EOS: HANTS (a), AG function (b), DL (c), SG filter (d), mean (e), and its standard deviation (f) for the four EOS dates. The top left inset shows the percentage of each interval in which the value was indicated by the map legend.**

This article has been accepted for publication in a future issue of this journal, but has not been fully edited. Content may change prior to final publication. Citation information: DOI 10.1109/ACCESS.2020.3043788, IEEE Access

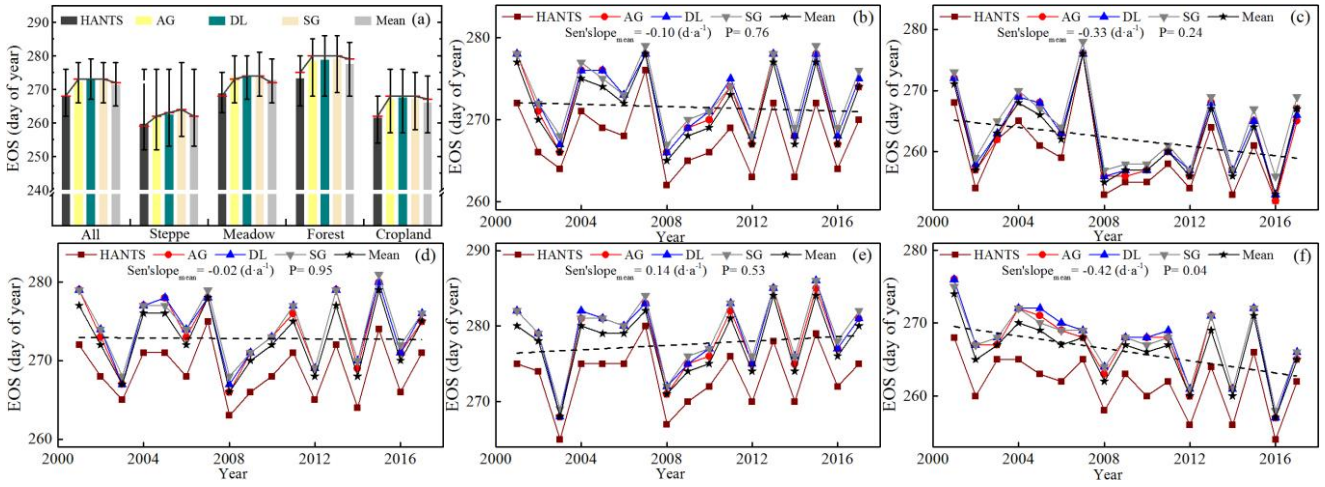

FIGURE 4. Average dates and standard deviation of EOS for the four smoothing methods and their mean (a). The interannual variations of EOS using the four smoothing methods (HANTS, AG, DL and SG) and mean EOS from 2001–2017 for entire study area (b), steppe (c), meadow (d), forest (e), and cropland (f).

B. SPATIAL DIFFERENCES AND TEMPORAL TRENDS

The spatial distribution of multiyear average EOS is shown in Fig. 3e. The EOS was in the range of days 240–300 (late August to late October). The earlier EOS dates, ranging from days 240 to 270, were mainly located in the southwestern and eastern parts of NIM. The central and northern regions had EOS dates ranging from days 270–300. In addition, we found that the spatial average EOS date in NIM was around day 271 ± 7 (late September) (Fig. 4a). In terms of plant functional types, the earliest EOS dates were observed in steppe (day 262 ± 14) and cropland (day 266 ± 10), while later EOS dates were found in meadows (day 273 ± 9) and forest (day 278 ± 6). Fig 4b-f shows the interannual changes of EOS during the period of 2001–2017, and clearly shows discrepancies in the EOS trends for different biomes. At the regional level, the EOS across the NIM displayed no significant advancing trend, with a rate of 0.1 $d \cdot a^{-1}$ (P = 0.76) (Fig. 4b). The EOS of steppe and cropland experienced advancing trends at rates of 0.33 $d \cdot a^{-1}$ (P = 0.24) and 0.42 $d \cdot a^{-1}$ (P = 0.04), respectively (Fig. 4c and f). The EOS of forest biome was delayed by 0.14 $d \cdot a^{-1}$ (Fig. 4e), but the delaying trend was not significant (P = 0.53). For the meadow ecosystem, there was no obvious trend (Sen's slope = -0.02 P = 0.95) in the EOS (Fig. 4d). We mapped the spatial distributions of EOS trends for the study period (Fig. 5). Over the study area, an advance of the EOS was observed across more than 63.7% of the total pixels, although it was significant in only 5.42% of the pixels, and the advance was more pronounced in the east of the Greater Khingan Mountains and western steppe area of NIM. In contrast, a delay in the EOS was observed in 36.3% of all pixels (significant in 3.86% of pixels), which were generally concentrated in the northern Greater Khingan Mountains.

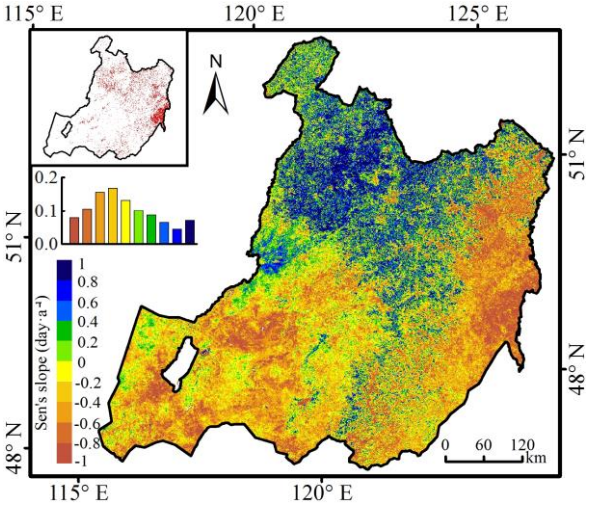

FIGURE 5. The trend of multimethod averaged EOS in NIM during 2001–2017 (the top left (upper) inset shows the pixels significant at p <0.05, the top left (lower) inset shows the percentage of each interval that is indicated on the map).

C. RESPONSES OF THE EOS TO POTENTIAL DRIVING FACTORS

1) RESPONSES OF THE EOS TO MULTIPLE CLIMATE FACTORS

At the regional scale, both T_{min} (R = 0.27, p >0.05) and T_{max} (R = 0.41, P >0.05) exhibited a positive influence on the EOS of the NIM, which occurred approximately at preseason day 80 (Fig. S3). In addition, the correlation between SSD and EOS was in general similar to the corresponding correlations found for T_{min} and T_{max} (Fig. S3), implying that a longer SSD was conducive to vegetation growth in autumn. However, the preseason length of SSD which had the strongest effect on the EOS was generally longer than the preseason length of T_{min} and T_{max}. In contrast, negative relationships between the EOS and both RHU (R = -0.46) and precipitation (R = -0.62) were observed (Fig. S3). These results implied that the EOS of NIM advanced under

This article has been accepted for publication in a future issue of this journal, but has not been fully edited. Content may change prior to final publication. Citation information: DOI 10.1109/ACCESS.2020.3043788, IEEE Access

increased RHU and precipitation. The strongest impacts of RHU and precipitation on the EOS mainly occurred in the short-term, within 10 days of the preseason. Biome-specific correlations between the EOS and preseason climate factors are presented in Fig. 6. It can be clearly seen that the relationship between the EOS and T_{min} varied substantially among the plant functional types. The EOS of steppe (R = 0.46, P >0.05) and meadow (R = 0.26, P >0.05) were positively correlated with T_{min}. In contrast, a negative correlation was found in forest (R = -0.38, P >0.05) and cropland (R = -0.44, P >0.05) regions. In general, the EOS for steppe and meadow would be delayed with a T_{min} increase, but it would advance with a T_{min} increase in the forest and cropland biomes. It was apparent that T_{max} had a positive impact in most subregions, except for the cropland (R = -0.41, P >0.05) area. The forest EOS was significantly related to T_{max} (R = 0.54, P <0.05). This indicates that a rising T_{max} was beneficial to vegetation growth for most vegetation types, especially in the forest region, but it restricted the growth of cropland in autumn. Furthermore, the EOS of all biomes were positively correlated with SSD, particularly for the forest (R = 0.53, P <0.05) and cropland (R = 0.51, P <0.05) areas. However, the EOS dates in all subregions were negatively correlated with RHU and precipitation.

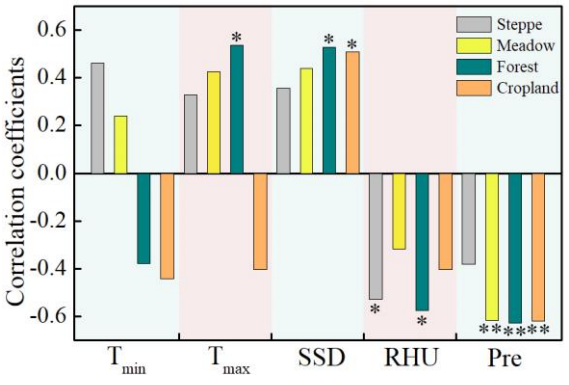

FIGURE 6. Correlation coefficients between the annual changes of the EOS with minimum temperature (T_{min}), maximum temperature (T_{max}), sunshine duration (SSD), relative humidity (RHU), and precipitation in NIM from 2001 to 2017. *and ** indicate significance at p <0.05 and p <0.01, respectively.

To determine the effects of climate factors on the EOS at the pixel scale, the correlation coefficients between the EOS and preseason climate factors were calculated (Fig. 7a-f). Across the study area, the EOS was positively correlated with T_{min} in 48.59% of the pixels in the total area (significant in 11.96% of pixels), and there was a negative correlation in 51.41% of pixels (significant in 12.91% of pixels). The EOS was positively correlated with T_{max} in most pixels (74.17%), with the correlation being significant for 21.66% of total pixels (Fig. 7f). In most pixels (74.08%) there was a positive correlation between SSD and the EOS throughout the NIM, with 24.78% being significant. In the remaining pixels, which represented 25.92% of the total areas, there was a negative correlation (Fig. 7f). Compared with the SSD, the opposite pattern was observed in the relationship between the EOS and both RHU and precipitation. Specifically, the EOS across NIM was negatively correlated with RHU and precipitation in 82.77% and 84.03% of all pixels, of which 31.52% and 40.21% were significant at the 0.05 level, respectively (Fig. 7f). Additionally, the EOS of NIM was most closely associated with T_{min} and T_{max} during the period of days 10–110, and the mid-value occurred at days 60 and 80, respectively (Fig. S4). In contrast, the preseason durations of SSD, RHU, and precipitation were concentrated over shorter time scales, with the mid-values mostly occurring at about day 30 (Fig. S4). In line with the across-biome results reported above, more than 70% of pixels had a positive correlation between the EOS and T_{max} for each biome, except cropland (Fig. 7b-f). The relationship between the EOS of cropland and T_{max} was ambiguous, with positive and negative correlations in 44.96% and 55.04% of all pixels, respectively. There was a positive correlation between SSD and the EOS in more than 63% of each biome, and around 30% of these positive correlations were significant at the 0.05 level, except for the steppe (significant in 7.35%) and meadow (significant in 16.25%) regions (Fig. 7f). Consistent results were also found for RHU and precipitation, with a negative correlation between the EOS with RHU and precipitation observed at more than 68% of pixels for each vegetation type, and most were significant in more than 20% of pixels (Fig. 7f). Compared with the factors mentioned above, there were large differences in the effects of T_{min} on the EOS among the different vegetation types. For steppe, more than 86% of the pixels had a positive correlation, and about 30% of the pixels were significant at the 0.05 level (Fig. 7f). With regard to forest and cropland areas, negative correlations between the EOS and T_{min} were observed in 63.81% (forest) and 75.31% (cropland) of pixels (Fig. 7f). The meadow EOS was positively correlated with T_{min} in 48.97% of pixels and negatively correlated with T_{min} in 51.03% of pixels, although the correlation was not significant in most pixels (Fig. 7f). Overall, the EOS of NIM was most strongly related to precipitation (Fig. 7a, Fig. S5), with an average correlation coefficient of -0.33, suggesting that the precipitation was the dominant climate factor controlling the variation of EOS. Consistent results were also found for meadow, forest, and cropland, with average correlation coefficients of -0.36, -0.44 and -0.33, respectively (Fig. 7c-e, Fig. S5). For steppe, both T_{min} and RHU were the driving climate factors that best explained the trend of EOS, with average correlation coefficients of 0.33 and -0.33, respectively (Fig. 7b, Fig. S5). Although the other climatic variables were selected in relatively few pixels, their influences on the EOS could not be ignored.

This article has been accepted for publication in a future issue of this journal, but has not been fully edited. Content may change prior to final publication. Citation information: DOI 10.1109/ACCESS.2020.3043788, IEEE Access

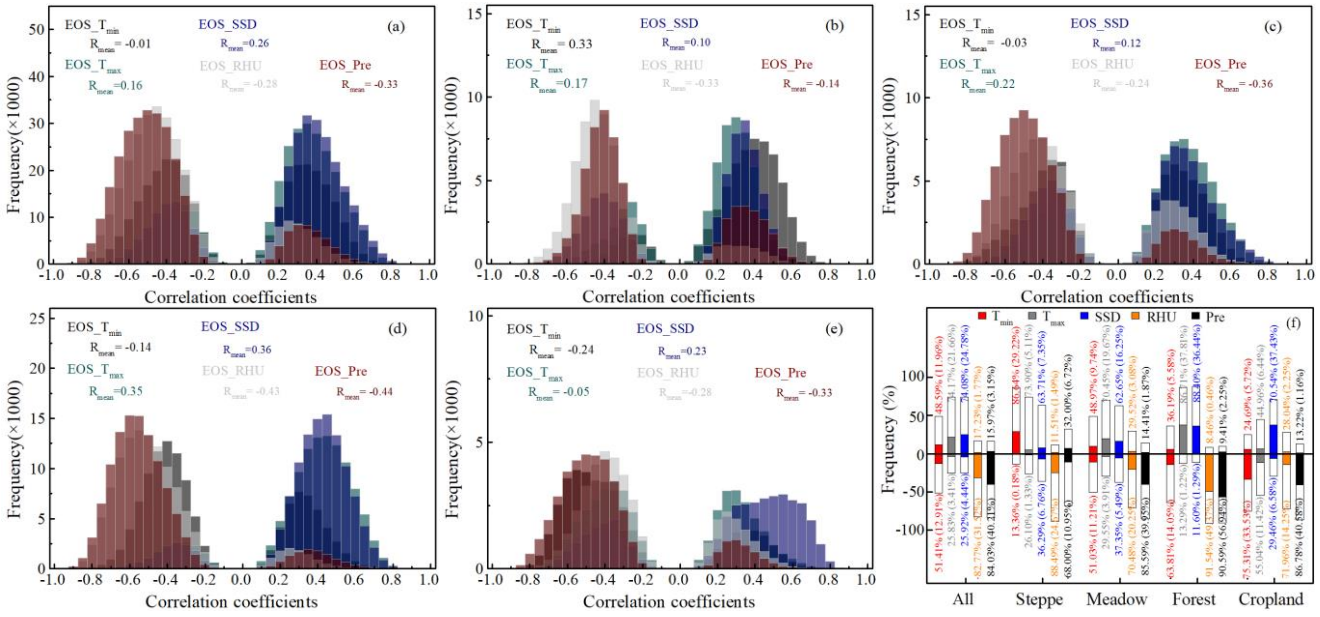

FIGURE 7. The frequency distribution of correlation coefficients between the EOS and climate factors: entire study area (a), steppe (b), meadow (c), forest (d), and cropland (e), and the percentages of correlation coefficients (f: bars above zero line represent percentage of positive correlations, and the underneath show negative percentages, colored sections show the percentage of significant correlations at $p < 0.05$).

2) RESPONSES OF THE EOS TO VEGETATION GROWTH AND THE POS

The spatial patterns of correlation between the EOS and both summer average NDVI and POS are shown in Fig. 8. We found that a positive correlation between the EOS and summer average NDVI was distributed in the northern and northeastern parts of NIM (52.17% of total pixels), while a negative correlation was identified in 47.83% of pixels (Fig. 8a). The spatial distribution of the relationship between the EOS and POS had the opposite sign to the relationship between summer average NDVI and EOS in most pixels (Fig. 8b). The EOS was negatively correlated with the POS in 51.53% of pixels and positively correlated with the POS in 48.47% of pixels in the NIM.

For steppe and cropland regions, the EOS was mainly negatively correlated with summer average NDVI in 77.03% and 63.47% of their total areas, with average correlation coefficients of -0.15 and -0.11, respectively (Fig. 8c, d). In contrast, the EOS was positively correlated with the POS in 78.39% and 65.46% of pixels, with average correlation coefficients of 0.18 and 0.13, respectively. This suggests that the EOS of steppe and cropland would advance with an increase in the summer average NDVI and an advance in the POS in most pixels. However, the summer average NDVI had a positive (67.00% of pixels) impact on the forest EOS, with an average correlation coefficient of 0.13, and the POS had a negative (64.75% of pixels) impact on the forest EOS, with an average correlation coefficient of -0.12 (Fig.8c, d). This indicated that the forest EOS would be delayed with the growth of vegetation in summer and an advanced POS. In addition, the response of meadow EOS on the summer average NDVI and POS were ambiguous (Fig. 8c, d), with a positive/negative correlation of the EOS with summer average NDVI of 58.39% / 41.61%, respectively. The meadow EOS was positively correlated with the POS in 40.58% of pixels and negatively correlated in 59.42% of pixels. Furthermore, we obtained the relationship between the EOS and NDVI for each summer month and September. For the entire study area, we found that the EOS was negatively correlated with the NDVI in June and July, while it was positively correlated with the NDVI in August and September (Fig. S6a). A similar pattern was observed in steppe and cropland regions (Fig. S6b, e). This implied that the vegetation activity in early summer would restrict the growth of autumn vegetation, while vegetation activity in late summer and early autumn would delay the vegetation degradation. For the meadow and forest areas, the NDVI had a positive effect on the EOS in all months, especially in August and September (Fig. S6c, d), indicating that the NDVI in all periods prior to leaf senescence was sufficient to promote vegetation growth in autumn and delay the EOS.

IV. DISCUSSION

A. RESPONSES OF DIFFERENT SMOOTHING METHODS ON THE EXTRACTION OF THE EOS

Numerous studies have concluded that all smoothing methods can effectively remove the residual noise in the NDVI [18], but the different methods produce differences in the description of overall trend of vegetation dynamics [48] and in the retention of details of seasonality signals [49]. In this study, we adopted the four frequently-used methods (HANTS, AG, DL, and SG) to smooth the time series of NDVI data and then extracted the EOS in NIM during the period of 2001–2017. The results of the comparison showed that the spatial distributions of the EOS retrieved from the different smoothing methods displayed similar patterns and the SDs were mainly within 6 days (Fig. 3f). This was inconsistent with previous studies in which large disparities (range of days 20–50) were reported in the SOS and length of

This article has been accepted for publication in a future issue of this journal, but has not been fully edited. Content may change prior to final publication. Citation information: DOI 10.1109/ACCESS.2020.3043788, IEEE Access

growing season (LOS) and that the SG filter was more reliable than the AG and DL for temperate grassland [27]. Several researchers have reported that the effects of smoothing methods on the estimation of land surface phenology vary greatly for different levels of vegetation coverage [24], [26]. In contrast, our study found that the EOS dates using different smoothing methods were similar at sample sites with different vegetation types (Fig. 2). The average SDs were relatively smaller in steppe (2 days) than the other biomes (4 days) at the pixel scale (Fig. S2). The differences in errors among the vegetation types may be caused by the signal to noise ratio of the NDVI time series, which is proportional to the confidence level for clear sky labeling [50]. Furthermore, Cong et al. [28] considered that the interannual changes of the EOS were mainly dependent on the smoothing method rather than the identification method, and found an obvious distinction between the Tibetan Plateau EOS trends based on the cubic spline and HANTS functions. Liu and Zhan. [51] also found that the DL function was better than the SG filter for describing the overall trend of the SOS. However, our results showed that the interannual variations of the EOS using various filter were in good agreement with each other for all biomes (Fig. 4), indicating that the use of different smoothing methods had little impact on the EOS trend in NIM. The inconsistency in the results of the different studies may be attributed to the differences in the methodology of phenology extraction [19], land surface conditions [28], and data resolution [52], [53].

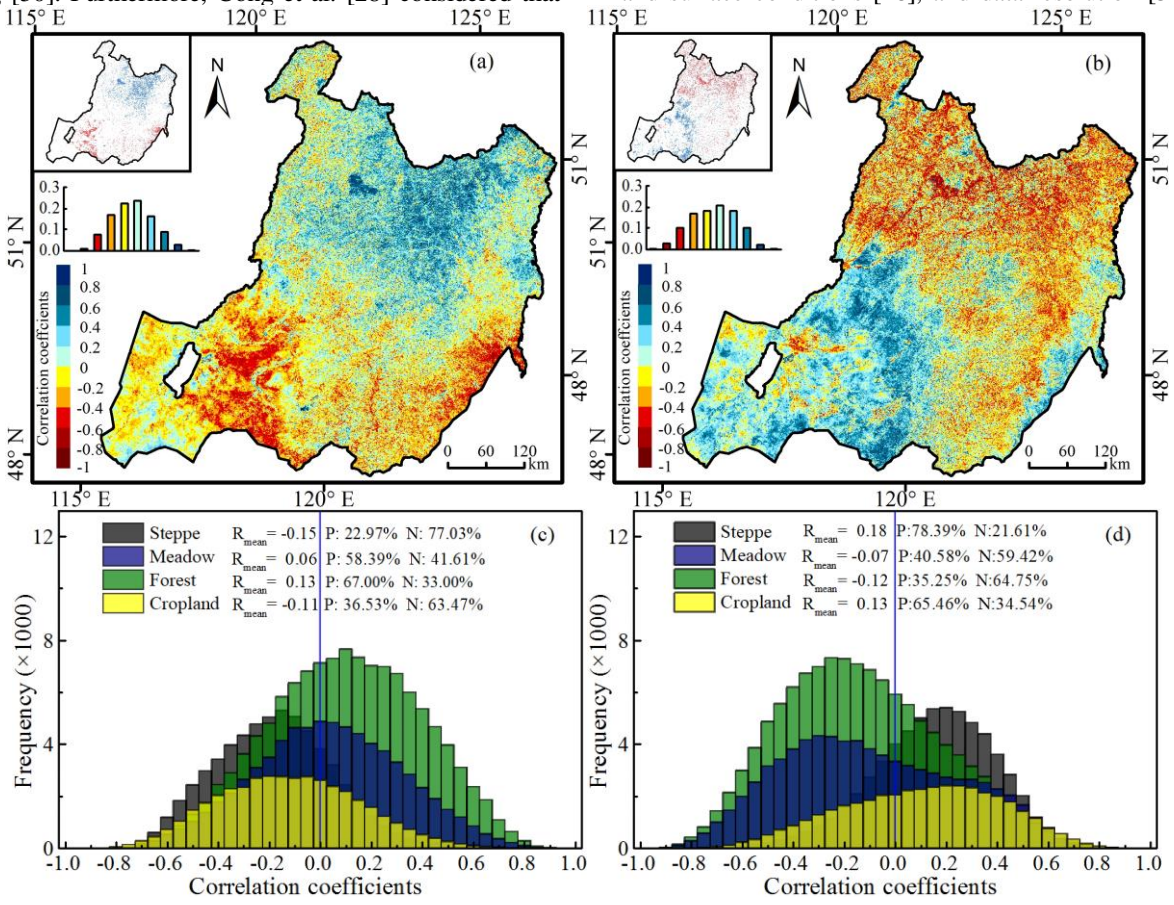

FIGURE 8. **Spatial pattern of the correlation coefficients of the EOS to summer NDVI (a), and peak of growing season (POS) (b), (The red (negative) and blue (positive) pixels in the top-left (upper) inset indicate significance at p <0.05; the top left inset (lower) shows the percentage of each interval that is indicated on the map legend). The frequency distribution of the correlation coefficients between the EOS and summer average NDVI (c) and POS (d) for different vegetation types, (P and N represent the positive and negative correlations, respectively).**

B. SPATIAL DIFFERENCES AND TEMPORAL TRENDS

Our results showed that the EOS ranged between days 240 and 300 (Fig. 3e), which was in agreement with previous studies that found the EOS mainly occurred in late-August to mid-October in the Mongolian Plateau [16] and temperate China [19], including NIM. Despite there being no clear patterns along the latitudinal or longitudinal gradients, the EOS of NIM displayed a spatial heterogeneity among the different vegetation types, with the forest EOS always being later than in steppe and meadow regions. This discrepancy may be attributed to plant functional types [54]. For example, the forest vegetation was more cold-resistant than the grassland as the temperature fell in autumn, therefore, leaf senescence occurred later in forest than in steppe and meadow areas [15].

In addition, this study identified a slight but non-significant advancing trend in the EOS of NIM during the

past 17 years (Fig. 4). The absence of an EOS tendency was mainly due to the offsetting effect caused by spatial variations [28], [35]. Our study observed that the forest EOS was delayed with a rate of 0.14 $d \cdot a^{-1}$. The delaying trend was consistent with previous results reported in forests in the eastern United States and semi-arid mountains of China, but its magnitude was different between arid and humid areas [56]–[58]. In contrast, the EOS of steppe displayed an advanced trend at a rate of 0.33 $d \cdot a^{-1}$, and the meadow EOS had a slightly earlier trend (0.02 $d \cdot a^{-1}$). This advancing trend of grassland was consistent with previous studies. For example, Bao *et al.* [16] investigated the EOS of the Mongolian Plateau over a long observation period and found an earlier trend in grassland areas. Liu *et al*. [19] studied the variation of the EOS from 1982–2011 in temperate China and observed an advancing trend (0.02 ± 0.01 $d \cdot a^{-1}$) in grassland areas of Inner Mongolia. However, a delaying trend of the EOS was reported in some other studies. Gong *et al.* [59] found that the EOS over the entire Inner Mongolia grassland during 2002–2014 was delayed at a rate of 0.51 $d \cdot a^{-1}$. Yang *et al.*[60] found that the EOS of temperate grassland in China was delayed by 0.08 $d \cdot a^{-1}$ during 1982–2010. The different rates of change and diverse EOS trends in grassland might be due to the different types of grassland, target periods, data resolution, and extraction methods.

C. RESPONSES OF THE EOS TO POTENTIAL DRIVING FACTORS

Previous studies have reported differential warming in recent decades in terms of T_{min} and T_{max}, which had asymmetric effects on the land surface phenology [2], [15], [30]. However, we found an equal effect of T_{min} and T_{max} on the EOS for steppe and meadow areas, with an increase in both T_{min} and T_{max} delaying the EOS (Fig. 6). These positive correlations may be partly due to the fact that a higher T_{min} could eliminate the risk of frost damage in autumn and slow the degradation of chlorophyll in plants [32]. An increase in T_{max} could enhance vegetation photosynthesis with the decline in temperature in autumn and postpone the EOS date [28], [61]. Although T_{min} is considered to be strongly related to the frequency of chilling damage in the boreal ecosystem [62], [63], our study identified a negative correlation between T_{min} and the EOS of the forest and cropland biomes (Fig. 6). An increased nighttime temperature would strengthen leaf respiration, consume large amounts of leaf carbohydrates, and then accelerate the development of autumn leaf coloration[30], [64]. This mechanism could partly explain the negative impact of T_{min} on the EOS. It should be noted that the cropland EOS was negatively correlated with T_{max}, which was mainly ascribed to the fact that a higher T_{max} may lead to decreasing the water content in the soil and restraining the vegetation growth in the irrigated agricultural area [65]. Significantly, there were great uncertainties in the relationship between the cropland EOS and climate factors due to this particular region being extraordinarily vulnerable to human management, such as changes in crop variety, irrigation, and fertilizers [66]. In most boreal and wet temperate regions, the vegetation growth was more sensitive to the photoperiod due to the seasonal temperature varying strongly [67]. Our results showed that the SSD had a positive effect on EOS for all biomes (Fig. 6). This was mainly because a longer SSD would stimulate the photosynthesis capacity of plants and thereby slow the speed of vegetation degradation [35], [68]. Additionally, we found that the EOS was negatively correlated with both RHU and precipitation for all biomes. This phenomenon may be explained by the fact that increasing precipitation was associated with lower radiation [15], and a higher RHU could result in a higher risk of freezing injury with the drop in autumn temperature in colder areas, subsequently promoting leaf senescence in autumn[60], [69].

Plants of each life-cycle rely heavily on their previous growth stage [37], [70]. For the steppe, we found that summer vegetation growth had a negative effect on the EOS (Fig. 8c), which was in accordance with the previous study in the alpine vegetation of the Tibetan Plateau [35]. This may be caused by the vigorous vegetation growth in summer being accompanied by the over consumption of soil water, thus, resulting in an earlier EOS for water-limited ecosystem [71]. The steppe vegetation grew fastest in June and needed more water at this time [72], and therefore the EOS of steppe was most strongly related to the NDVI in June (Fig. S6b). Interestingly, the forest EOS was positively correlated with the NDVI in months prior to the EOS and most strongly related to September NDVI (Fig. S6d). This suggests that vegetation growth in all periods prior to leaf senescence would delay the EOS, especially in the autumn. Compared with herbaceous plants, woody plants with developed roots are habituated to uptake deeper soil water [20], resulting in less dependence on land surface water variability. Additionally, woody plants are likely to be more drought resistant than herbaceous plants due to their ability to store water [20]. Additionally, strong preseason vegetation activity indicates an improvement in carbon sequestration [13]. As a result, vegetation growth in the preceding stage would slow the rate of leaf senescence and postpone the forest EOS. Furthermore, with the decline in autumn temperature, the stronger photosynthetic capacity of vegetation would have a heat preservation function, keeping the land surface temperature relatively stable in autumn[73]. This phenomenon could explain the strongest impact of NDVI on the forest EOS being strongest in September. Cong *et al.*[28] demonstrated that plants with a shorter growing season have lower plasticity in regulating the length of growing season and have a more conservative strategy. Thus, an earlier or later peak season activity is accompanied by advanced or delayed degradation of vegetation with a shorter length of growing season [74]. These results may help to explain the positive correlation between the POS and EOS in steppe and cropland areas (Fig. 8d). Nevertheless, there were negative effects of the POS on forest and meadow EOS, which could be attributed to several factors. First, the forest and meadow plants with a longer growing season had a higher plasticity in adjusting their life-cycle stage and were more sensitive to

preseason climate factors [75]. Furthermore, the earlier POS enabled the vegetation to assimilate more carbon [76] and accelerated vegetation photosynthesis in autumn [12].

V. CONCLUSION

The reliable detection and attribution of variations in the EOS are the prerequisites for simulating ecosystem carbon cycle processes under climate change. This study provided an important comparative analysis of the effect of four smoothing methods on the extraction of the EOS for different plant functional types. Overall, there was a fairly good agreement among the EOS dates obtained with the four smoothing methods in terms of their representation of spatial patterns and interannual variations. Furthermore, we found advancing trends of EOS in the grassland and cropland regions, and an extensive delayed trend in the forest region during the period of 2001-2017. Our study also revealed that T_{min}, T_{max}, and SSD exerted positive effects on the EOS trends across the NIM, while an increase in RHU and precipitation would lead to an earlier EOS. We further investigated the relationship between EOS and both vegetation growth in the period before the EOS and POS, and found a heterogeneous spatial pattern. Summer vegetation growth generally advanced the steppe EOS, while delayed the EOS of meadow and forest regions. In addition, an earlier POS would advance the EOS of steppe, but the relationship was the opposite in meadow and forest areas. These observations indicated that climate factors and the preceding growth stage of vegetation jointly determined the variation of EOS in the NIM. Future studies are needed to investigate the potential interactions between the environmental controlling factors and to develop a full understanding of the mechanisms influencing the autumn phenology.

REFERENCES

[1] A. D. Richardson, D. Y. Hollinger, D. B. Dail, J. T. Lee, J. W. Munger, and J. O'keefe, "Influence of spring phenology on seasonal and annual carbon balance in two contrasting New England forests," Tree Physiology, vol. 29, no. 3, Art. no. 3, Jan. 2009, doi: 10.1093/treephys/tpn040.

[2] S. Piao et al., "Leaf onset in the northern hemisphere triggered by daytime temperature," Nat Commun, vol. 6, no. 1, Art. no. 1, Nov. 2015, doi: 10.1038/ncomms7911.

[3] S.-J. Jeong, C.-H. Ho, and J.-H. Jeong, "Increase in vegetation greenness and decrease in springtime warming over east Asia: VEGETATION WEAKEN REGIONAL WARMING," Geophys. Res. Lett., vol. 36, no. 2, Art. no. 2, Jan. 2009, doi: 10.1029/2008GL036583.

[4] R. John et al., "Differentiating anthropogenic modification and precipitation-driven change on vegetation productivity on the Mongolian Plateau," Landscape Ecol, vol. 31, no. 3, Art. no. 3, Mar. 2016, doi: 10.1007/s10980-015-0261-x.

[5] Q. Du, H. Liu, Y. Li, L. Xu, and S. Diloksumpun, "The effect of phenology on the carbon exchange process in grassland and maize cropland ecosystems across a semiarid area of China," Science of The Total Environment, vol. 695, p. 133868, Dec. 2019, doi: 10.1016/j.scitotenv.2019.133868.

[6] R. B. Myneni, C. D. Keeling, C. J. Tucker, G. Asrar, and R. R. Nemani, "Increased plant growth in the northern high latitudes from 1981 to 1991," Nature, vol. 386, no. 6626, Art. no. 6626, Apr. 1997, doi: 10.1038/386698a0.

[7] J. T. Morisette et al., "Tracking the rhythm of the seasons in the face of global change: phenological research in the 21st century," Frontiers in Ecology and the Environment, vol. 7, no. 5, Art. no. 5, Jun. 2009, doi: 10.1890/070217.

[8] C. J. Tucker, D. A. Slayback, J. E. Pinzon, S. O. Los, R. B. Myneni, and M. G. Taylor, "Higher northern latitude normalized difference vegetation index and growing season trends from 1982 to 1999," International Journal of Biometeorology, vol. 45, no. 4, Art. no. 4, Nov. 2001, doi: 10.1007/s00484-001-0109-8.

[9] A. Gonsamo, J. M. Chen, D. T. Price, W. A. Kurz, and C. Wu, "Land surface phenology from optical satellite measurement and CO 2 eddy covariance technique: LAND SURFACE PHENOLOGY INDEX," J. Geophys. Res., vol. 117, no. G3, Art. no. G3, Sep. 2012, doi: 10.1029/2012JG002070.

[10] S. Piao et al., "Plant phenology and global climate change: Current progresses and challenges," Glob Change Biol, vol. 25, no. 6, Art. no. 6, Jun. 2019, doi: 10.1111/gcb.14619.

[11] A. Menzel et al., "European phenological response to climate change matches the warming pattern," Global Change Biol, vol. 12, no. 10, Art. no. 10, Oct. 2006, doi: 10.1111/j.1365-2486.2006.01193. x.

[12] C. Xu, H. Liu, A. P. Williams, Y. Yin, and X. Wu, "Trends toward an earlier peak of the growing season in Northern Hemisphere mid-latitudes," Glob Change Biol, vol. 22, no. 8, Art. no. 8, Aug. 2016, doi: 10.1111/gcb.13224.

[13] J. Tao et al., "Elevation-dependent effects of growing season length on carbon sequestration in Xizang Plateau grassland," Ecological Indicators, vol. 110, p. 105880, Mar. 2020, doi: 10.1016/j.ecolind.2019.105880.

[14] S. Piao et al., "Net carbon dioxide losses of northern ecosystems in response to autumn warming," Nature, vol. 451, no. 7174, Art. no. 7174, Jan. 2008, doi: 10.1038/nature06444.

[15] C. Wu et al., "Contrasting responses of autumn-leaf senescence to daytime and night-time warming," Nature Clim Change, vol. 8, no. 12, Art. no. 12, Dec. 2018, doi: 10.1038/s41558-018-0346-z.

[16] G. Bao et al., "Dynamics of net primary productivity on the Mongolian Plateau: Joint regulations of phenology and drought," International Journal of Applied Earth Observation and Geoinformation, vol. 81, pp. 85–97, Sep. 2019, doi: 10.1016/j.jag.2019.05.009.

[17] Y. Ni, Y. Zhou, and J. Fan, "Characterizing Spatiotemporal Pattern of Vegetation Greenness Breakpoints on Tibetan Plateau Using GIMMS NDVI3g Dataset," IEEE Access, vol. 8, pp. 56518–56527, 2020, doi: 10.1109/ACCESS.2020.2982661.

[18] J. Zhou, L. Jia, M. Menenti, and B. Gorte, "On the performance of remote sensing time series reconstruction methods – A spatial comparison," Remote Sensing of Environment, vol. 187, pp. 367–384, Dec. 2016, doi: 10.1016/j.rse.2016.10.025.

[19] Q. Liu, Y. H. Fu, Z. Zeng, M. Huang, X. Li, and S. Piao, "Temperature, precipitation, and insolation effects on autumn vegetation phenology in temperate China," Glob Change Biol, vol. 22, no. 2, Art. no. 2, Feb. 2016, doi: 10.1111/gcb.13081.

[20] J. Peng, C. Wu, X. Zhang, X. Wang, and A. Gonsamo, "Satellite detection of cumulative and lagged effects of drought on autumn leaf senescence over the Northern Hemisphere," Glob Change Biol, vol. 25, no. 6, Art. no. 6, Jun. 2019, doi: 10.1111/gcb.14627.

[21] J. Chen, Per. Jönsson, M. Tamura, Z. Gu, B. Matsushita, and L. Eklundh, "A simple method for reconstructing a high-quality NDVI time-series data set based on the Savitzky–Golay filter," Remote Sensing of Environment, vol. 91, no. 3–4, Art. no. 3–4, Jun. 2004, doi: 10.1016/j.rse.2004.03.014.

[22] A. Moody and D. M. Johnson, "Land-Surface Phenologies from AVHRR Using the Discrete Fourier Transform," Remote Sensing of Environment, vol. 75, no. 3, Art. no. 3, Mar. 2001, doi: 10.1016/S0034-4257(00)00175-9.

[23] X. Zhang et al., "Monitoring vegetation phenology using MODIS," Remote Sensing of Environment, vol. 84, no. 3, Art. no. 3, Mar. 2003, doi: 10.1016/S0034-4257(02)00135-9.

[24] M. A. White et al., "Intercomparison, interpretation, and assessment of spring phenology in North America estimated from remote sensing for 1982-2006," Global Change Biology, vol. 15, no. 10, Art. no. 10, Oct. 2009, doi: 10.1111/j.1365-2486.2009.01910. x.

[25] N. Cong et al., "Spring vegetation green-up date in China inferred from SPOT NDVI data: A multiple model analysis," Agricultural and Forest Meteorology, vol. 165, pp. 104–113, Nov. 2012, doi: 10.1016/j.agrformet.2012.06.009.

[26] P. M. Atkinson, C. Jeganathan, J. Dash, and C. Atzberger, "Inter-comparison of four models for smoothing satellite sensor time-series data to estimate vegetation phenology," Remote Sensing of Environment, vol. 123, pp. 400–417, Aug. 2012, doi: 10.1016/j.rse.2012.04.001.

[27] B. Lara and M. Gandini, "Assessing the performance of smoothing functions to estimate land surface phenology on temperate grassland," International Journal of Remote Sensing, vol. 37, no. 8, Art. no. 8, Apr. 2016, doi: 10.1080/2150704X.2016.1168945.

[28] N. Cong, M. Shen, and S. Piao, "Spatial variations in responses of vegetation autumn phenology to climate change on the Tibetan Plateau," JPECOL, p. rtw084, Sep. 2016, doi: 10.1093/jpe/rtw084.

[29] IPCC, 2013. Climate Change 2013: The Physical Science Basis. Contribution of Working Group I to the Fifth Assessment Report of the Intergovernmental Panel on Climate Change. Cambridge University Press, Cambridge, UK

[30] S. Peng et al., "Asymmetric effects of daytime and night-time warming on Northern Hemisphere vegetation," Nature, vol. 501, no. 7465, Art. no. 7465, Sep. 2013, doi: 10.1038/nature12434.

[31] Y. H. Chew, A. M. Wilczek, M. Williams, S. M. Welch, J. Schmitt, and K. J. Halliday, "An augmented Arabidopsis phenology model reveals seasonal temperature control of flowering time," New Phytologist, vol. 194, no. 3, Art. no. 3, May 2012, doi: 10.1111/j.1469-8137.2012.04069. x.

[32] Z. Yang et al., "Asymmetric Responses of the End of Growing Season to Daily Maximum and Minimum Temperatures on the Tibetan Plateau: Autumn Phenology on Tibetan Plateau," J. Geophys. Res. Atmos., vol. 122, no. 24, Art. no. 24, Dec. 2017, doi: 10.1002/2017JD027318.

[33] J. Welty, S. Stillman, X. Zeng, and J. Santanello, "Increased Likelihood of Appreciable Afternoon Rainfall Over Wetter or Drier Soils Dependent Upon Atmospheric Dynamic Influence," Geophys. Res. Lett., vol. 47, no. 11, Art. no. 11, Jun. 2020, doi: 10.1029/2020GL087779.

[34] A. D. Richardson et al., "Terrestrial biosphere models need better representation of vegetation phenology: results from the North American Carbon Program Site Synthesis," Glob Change Biol, vol. 18, no. 2, Art. no. 2, Feb. 2012, doi: 10.1111/j.1365-2486.2011.02562. x.

[35] P. Li et al., "Dynamics of vegetation autumn phenology and its response to multiple environmental factors from 1982 to 2012 on Qinghai-Tibetan Plateau in China," Science of The Total Environment, vol. 637–638, pp. 855–864, Oct. 2018, doi: 10.1016/j.scitotenv.2018.05.031.

[36] M. Yuan, L. Zhao, A. Lin, Q. Li, D. She, and S. Qu, "How do climatic and non-climatic factors contribute to the dynamics of vegetation autumn phenology in the Yellow River Basin, China" Ecological Indicators, vol. 112, p. 106112, May 2020, doi: 10.1016/j.ecolind.2020.106112.

[37] J. Zu, Y. Zhang, K. Huang, Y. Liu, N. Chen, and N. Cong, "Biological and climate factors co-regulated spatial-temporal dynamics of vegetation autumn phenology on the Tibetan Plateau," International Journal of Applied Earth Observation and Geoinformation, vol. 69, pp. 198–205, Jul. 2018, doi: 10.1016/j.jag.2018.03.006.

[38] A. Gonsamo, J. M. Chen, and Y. W. Ooi, "Peak season plant activity shift towards spring is reflected by increasing carbon uptake by extratropical ecosystems," Glob Change Biol, vol. 24, no. 5, Art. no. 5, May 2018, doi: 10.1111/gcb.14001.

[39] T. Park et al., "Changes in timing of seasonal peak photosynthetic activity in northern ecosystems," Glob Change Biol, p. gcb.14638, May 2019, doi: 10.1111/gcb.14638.

[40] J. Chen et al., "Policy shifts influence the functional changes of the CNH systems on the Mongolian plateau," Environ. Res. Lett., vol. 10, no. 8, Art. no. 8, Aug. 2015, doi: 10.1088/1748-9326/10/8/085003.

[41] J. Chen et al., "Prospects for the sustainability of social-ecological systems (SES) on the Mongolian plateau: five critical issues," Environ. Res. Lett., vol. 13, no. 12, Art. no. 12, Dec. 2018, doi: 10.1088/1748-9326/aaf27b.

[42] G. Q. Tabios and J. D. Salas, "A COMPARATIVE ANALYSIS OF TECHNIQUES FOR SPATIAL INTERPOLATION OF PRECIPITATION," J Am Water Resources Assoc, vol. 21, no. 3, Art. no. 3, Jun. 1985, doi: 10.1111/j.1752-1688.1985. tb 00147.x.

[43] R. John, J. Chen, N. Lu, and B. Wilske, "Land cover/land use change in semi-arid Inner Mongolia: 1992–2004," Environ. Res. Lett., vol. 4, no. 4, Art. no. 4, Oct. 2009, doi: 10.1088/1748-9326/4/4/045010.

[44] J. Gu, X. Li, C. Huang, and G. S. Okin, "A simplified data assimilation method for reconstructing time-series MODIS NDVI data," Advances in Space Research, vol. 44, no. 4, Art. no. 4, Aug. 2009, doi: 10.1016/j.asr.2009.05.009.

[45] X. Hou, S. Gao, Z. Niu, and Z. Xu, "Extracting grassland vegetation phenology in North China based on cumulative SPOT-VEGETATION NDVI data," International Journal of Remote Sensing, vol. 35, no. 9, Art. no. 9, May 2014, doi: 10.1080/01431161.2014.903437.

[46] S. Piao, A. Mohammat, J. Fang, Q. Cai, and J. Feng, "NDVI-based increase in growth of temperate grasslands and its responses to climate changes in China," Global Environmental Change, vol. 16, no. 4, Art. no. 4, Oct. 2006, doi: 10.1016/j.gloenvcha.2006.02.002.

[47] P. K. Sen, "Estimates of the Regression Coefficient Based on Kendall's Tau," Journal of the American Statistical Association, vol. 63, no. 324, Art. no. 324, Dec. 1968, doi: 10.1080/01621459.1968.10480934.

[48] X. Wang and C. Wu, "Estimating the peak of growing season (POS) of China's terrestrial ecosystems," Agricultural and Forest Meteorology, vol. 278, p. 107639, Nov. 2019, doi: 10.1016/j.agrformet.2019.107639.

[49] R. Liu, R. Shang, Y. Liu, and X. Lu, "Global evaluation of gap-filling approaches for seasonal NDVI with considering vegetation growth trajectory, protection of key point, noise resistance and curve stability," Remote Sensing of Environment, vol. 189, pp. 164–179, Feb. 2017, doi: 10.1016/j.rse.2016.11.023.

[50] S. Kandasamy and R. Fernandes, "An approach for evaluating the impact of gaps and measurement errors on satellite land surface phenology algorithms: Application to 20year NOAA AVHRR data over Canada," Remote Sensing of Environment, vol. 164, pp. 114–129, Jul. 2015, doi: 10.1016/j.rse.2015.04.014.

[51] J. Liu and P. Zhan, "The impacts of smoothing methods for time-series remote sensing data on crop phenology extraction," in 2016 IEEE International Geoscience and Remote Sensing Symposium (IGARSS), Beijing, China, Jul. 2016, pp. 2296–2299, doi: 10.1109/IGARSS.2016.7729593.

[52] X. Wang et al., "No Consistent Evidence for Advancing or Delaying Trends in Spring Phenology on the Tibetan Plateau," J. Geophys. Res. Biogeosci., vol. 122, no. 12, Art. no. 12, Dec. 2017, doi: 10.1002/2017JG003949.

[53] Y. Zhu et al., "Effects of data temporal resolution on phenology extractions from the alpine grasslands of the Tibetan Plateau," Ecological Indicators, vol. 104, pp. 365–377, Sep. 2019, doi: 10.1016/j.ecolind.2019.05.004.

[54] C. Wu et al., "Land surface phenology derived from normalized difference vegetation index (NDVI) at global FLUXNET sites," Agricultural and Forest Meteorology, vol. 233, pp. 171–182, Feb. 2017, doi: 10.1016/j.agrformet.2016.11.193.

[55] G. Bao, Y. Bao, A. Sanjjava, Z. Qin, Y. Zhou, and G. Xu, "NDVI-indicated long-term vegetation dynamics in Mongolia and their response to climate change at biome scale: VEGETATION DYNAMICS IN MONGOLIA AND THEIR RESPONSE TO CLIMATE CHANGE," Int. J. Climatol., vol. 35, no. 14, Art. no. 14, Nov. 2015, doi: 10.1002/joc.4286.

[56] T. F. Keenan et al., "Net carbon uptake has increased through warming-induced changes in temperate forest phenology," Nature Clim Change, vol. 4, no. 7, Art. no. 7, Jul. 2014, doi: 10.1038/nclimate2253.

[57] J. Du, Z. He, J. Yang, L. Chen, and X. Zhu, "Detecting the effects of climate change on canopy phenology in coniferous forests in semi-arid mountain regions of China," International Journal of Remote Sensing, vol. 35, no. 17, Art. no. 17, Sep. 2014, doi: 10.1080/01431161.2014.955146.

[58] Z. He et al., "Assessing temperature sensitivity of subalpine shrub phenology in semi-arid mountain regions of China," Agricultural and Forest Meteorology, vol. 213, pp. 42–52, Nov. 2015, doi: 10.1016/j.agrformet.2015.06.013.

[59] Z. Gong et al., "MODIS normalized difference vegetation index (NDVI) and vegetation phenology dynamics in the Inner Mongolia grassland," Solid Earth, vol. 6, no. 4, Art. no. 4, Nov. 2015, doi: 10.5194/se-6-1185-2015.

[60] Y. Yang, H. Guan, M. Shen, W. Liang, and L. Jiang, "Changes in autumn vegetation dormancy onset date and the climate controls across temperate ecosystems in China from 1982 to 2010," Glob Change Biol, vol. 21, no. 2, Art. no. 2, Feb. 2015, doi: 10.1111/gcb.12778.

[61] C. Shi et al., "Effects of Warming on Chlorophyll Degradation and Carbohydrate Accumulation of Alpine Herbaceous Species during Plant Senescence on the Tibetan Plateau," PLoS ONE, vol. 9, no. 9, Art. no. 9, Sep. 2014, doi: 10.1371/journal.pone.0107874.

[62] O. Langvall and G. Örlander, "Effects of pine shelterwoods on microclimate and frost damage to Norway spruce seedlings," Can. J. For. Res., vol. 31, no. 1, Art. no. 1, Jan. 2001, doi: 10.1139/x00-149.

[63] M. Shen et al., "Strong impacts of daily minimum temperature on the green-up date and summer greenness of the Tibetan Plateau," Glob Change Biol, vol. 22, no. 9, Art. no. 9, Sep. 2016, doi: 10.1111/gcb.13301.

[64] K. L. Griffin et al., "Leaf respiration is differentially affected by leaf vs. stand-level night-time warming," Global Change Biol, vol. 8, no. 5, Art. no. 5, May 2002, doi: 10.1046/j.1365-2486.2002.00487. x.

[65] Y. Feng and X. Zhao, "Daily temperature trend and sensitivity to grassland and cropland in eastern China during the past 32 years: TEMPERATURE VARIABILITY AND ITS SENSITIVITY TO GRASSLAND AND CROPLAND," Int. J. Climatol., vol. 35, no. 7, Art. no. 7, Jun. 2015, doi: 10.1002/joc.4072.

[66] W. Wu, R. Shibasaki, P. Yang, Q. Zhou, and H. Tang, "Characterizing spatial patterns of phenology in China's cropland based on remotely sensed data," International Workshop on Earth Observation and Remote Sensing Applications, p. 6, 2008.

[67] X. Shen et al., "Spatiotemporal change of diurnal temperature range and its relationship with sunshine duration and precipitation in China," J. Geophys. Res. Atmos., vol. 119, no. 23, Art. no. 23, Dec. 2014, doi: 10.1002/2014JD022326.

[68] Y. Fracheboud, V. Luquez, L. Björkén, A. Sjödin, H. Tuominen, and S. Jansson, "The Control of Autumn Senescence in European Aspen," Plant Physiol., vol. 149, no. 4, Art. no. 4, Apr. 2009, doi: 10.1104/pp.108.133249.

[69] M. Yuan, L. Wang, A. Lin, Z. Liu, and S. Qu, "Variations in land surface phenology and their response to climate change in Yangtze River basin during 1982–2015," Theor Appl Climatol, vol. 137, no. 3–4, Art. no. 3–4, Aug. 2019, doi: 10.1007/s00704-018-2699-7.

[70] L. L. Jiang et al., "Relatively stable response of fruiting stage to warming and cooling relative to other phenological events," Ecology, vol. 97, no. 8, Art. no. 8, Aug. 2016, doi: 10.1002/ecy.1450.

[71] K. Zhang et al., "Vegetation Greening and Climate Change Promote Multidecadal Rises of Global Land Evapotranspiration," Sci Rep, vol. 5, no. 1, Art. no. 1, Dec. 2015, doi: 10.1038/srep15956.

[72] H. Wang et al., "Alpine grassland plants grow earlier and faster but biomass remains unchanged over 35 years of climate change," Ecol Lett, vol. 23, no. 4, pp. 701–710, Apr. 2020, doi: 10.1111/ele.13474.

[73] Q. Pang, L. Zhao, Y. Ding, and S. Li, "Analysis about the influence on the thermal regime in permafrost regions with different underlying surfaces," Sciences in Cold and Arid Regions, p. 9, 2010.

[74] Y. S. H. Fu et al., "Variation in leaf flushing date influences autumnal senescence and next year's flushing date in two temperate tree species," Proceedings of the National Academy of Sciences, vol. 111, no. 20, Art. no. 20, May 2014, doi: 10.1073/pnas.1321727111.

[75] Z. Shi, Y. Liu, and F. Wang, "Ecosystem Respiration under Different Mycorrhizal Strategy Dominated Forest and their Response to Temperature and Precipitation," p. 4, 2012.

[76] M. J. Duveneck and J. R. Thompson, "Climate change imposes phenological trade-offs on forest net primary productivity: Phenological Trade-Offs on Forests," J. Geophys. Res. Biogeosci., vol. 122, no. 9, Art. no. 9, Sep. 2017, doi: 10.1002/2017JG004025.

This article has been accepted for publication in a future issue of this journal, but has not been fully edited. Content may change prior to final publication. Citation information: DOI 10.1109/ACCESS.2020.3043788, IEEE Access

Wendu Rina received the M.S. degree in Cartography and Geography Information System from College of Geographical Science, Inner Mongolia Normal University, Hohhot, in 2017. She is currently pursuing the Ph.D. degree with the Inner Mongolia Normal University, Hohhot, China. Her research interests include vegetation dynamic monitoring and ecosystem response to climate change.

Gang Bao received the Ph.D. degree in Remote Sensing of Resources and Environment from International Institute for Earth System Science, Nanjing University, Nanjing, in 2016. He is currently the associate professor with the College of Geographical Science, Inner Mongolia Normal University, Hohhot. His research interests include vegetation dynamic monitoring and remote sensing applications.

Siqin Tong received the Ph.D. degree in Cartography and Geography Information System from School of Environment, Northeast Normal University, Changchun, in 2019. She is currently the associate Professor with the College of Geographical Science, Inner Mongolia Normal University, Hohhot. Her research interests include climate change monitoring and terrestrial ecosystems productivity simulation.

Yuhai Bao received the Ph.D. degree in Cartography and Geography Information System from Institute of Remote Sensing Applications, Chinese Academy of Sciences, Beijing, in 1999. He is currently the Dean and the Professor with the College of Geographical Science, Inner Mongolia Normal University, Hohhot. His research interests include 3S (GPS, GIS, and RS) integration and applications.

Yin Shan received the Ph.D. degree in Soil and Water Conservation and Desertification Combating from College of Ecological Environment, Inner Mongolia Agricultural University, Hohhot, in 2010. He is currently the Professor with the College of Geographical Science, Inner Mongolia Normal University, Hohhot. His research interests include desertification monitoring and assessment.

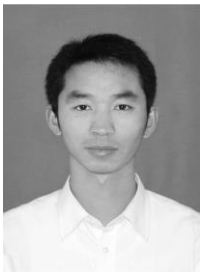

Xiaojun Huang received the Ph.D. degree in Cartography and Geography Information System from College of Earth and Environmental Sciences, Lanzhou University, Lanzhou, in 2019. He is currently a Professor with the College of Geographical Science, Inner Mongolia Normal University, Hohhot. His research interests include remote sensing monitoring of natural disasters and ecological environment.

Hong Ying received the M.S. degree in Cartography and Geography Information System from School of Geographical Sciences, Northeast Normal University, Changchun, in 2016. She is currently pursuing the Ph.D. degree with the Northeast Normal University, Changchun, China. Her research interests include climate change and vegetation remote sensing.

Lingtong Du received the Ph.D. degree in Remote Sensing of Resources and Environment from International Institute for Earth System Science, Nanjing University, Nanjing, in 2013. He is currently the professor with Breeding Base for State Key Laboratory of Land Degradation and Ecological Restoration in Northwest China, Ningxia University, Yinchuan. His research interests include remote sensing of environmental and spatial analysis.